# Enhancing the Signalling of GPCRs via Orthosteric Ions

H.C. Stephen Chan†#, Yueming Xu‡#, Liang Tan‡#, Horst Vogel†§, Jianjun Cheng‡*,

Dong Wu‡*, Shuguang Yuan†*

† Shenzhen Institutes of Advanced Technology, Chinese Academy of Sciences, Shenzhen 518055, China

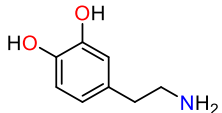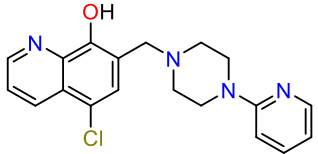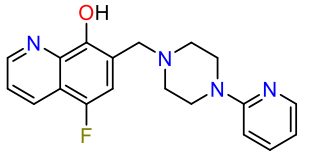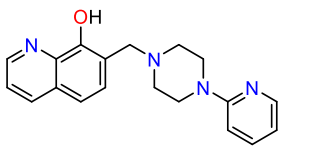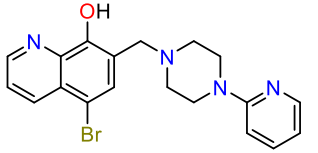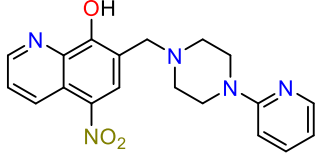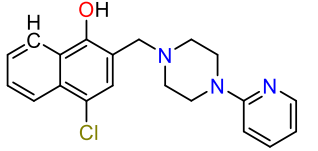‡iHuman Institute, ShanghaiTech University, Shanghai 201210, China

§Institute of Chemical Sciences and Engineering, Ecole Polytechnique Fédérale de Lausanne (EPFL), Lausanne 1015, Switzerland

Table-S1 Dopamine activation against D2R variants ($EC_{50}$, nM).

| Dopamine | WT | L94A | D114 | I183A | I184A | F389A | F390A | H393A |
|---|---|---|---|---|---|---|---|---|
| β-arrestin | 970±420 | 288±2 | N/A | N/A | 274±16 | 940±24 | N/A | 1002±87 |
| G protein | 2.2±0.15 | N/A | N/A | N/A | 588±324 | N/A | N/A | 39.8±19.6 |

Table-S2 Dopamine and MLS1547 derivatives against wild type D2R (EC$_{50}$, nM)

| Compounds | structure | G protein EC$_{50}$ (nM) | Arrestin EC$_{50}$ (nM) | pKa* | Calculated relative Binding energy(kcal/mol) |
|---|---|---|---|---|---|
| dopamine | | 2.2±0.2 | 970±420 | – | – |
| MLS1547 | | 290±90 | 250±60 | 6.3±0.8 | -16.6±0.6 |
| MLS-d1 | | 18.6 ± 3.1 | 68.8±1.4 | 4.2±0.4 | -20.4±0.8 |
| MLS-d2 | | 95±6 | 135±10 | 6.4±0.7 | -18.1±0.5 |
| MLS-d3 | | inactive | inactive | 7.4±0.5 | -10.0±0.8 |
| MLS-d4 | | inactive | inactive | 3.4±0.9 | -9.6±0.7 |
| MLS-d5 | | inactive | inactive | 6.9±0.6 | -8.2±0.7 |

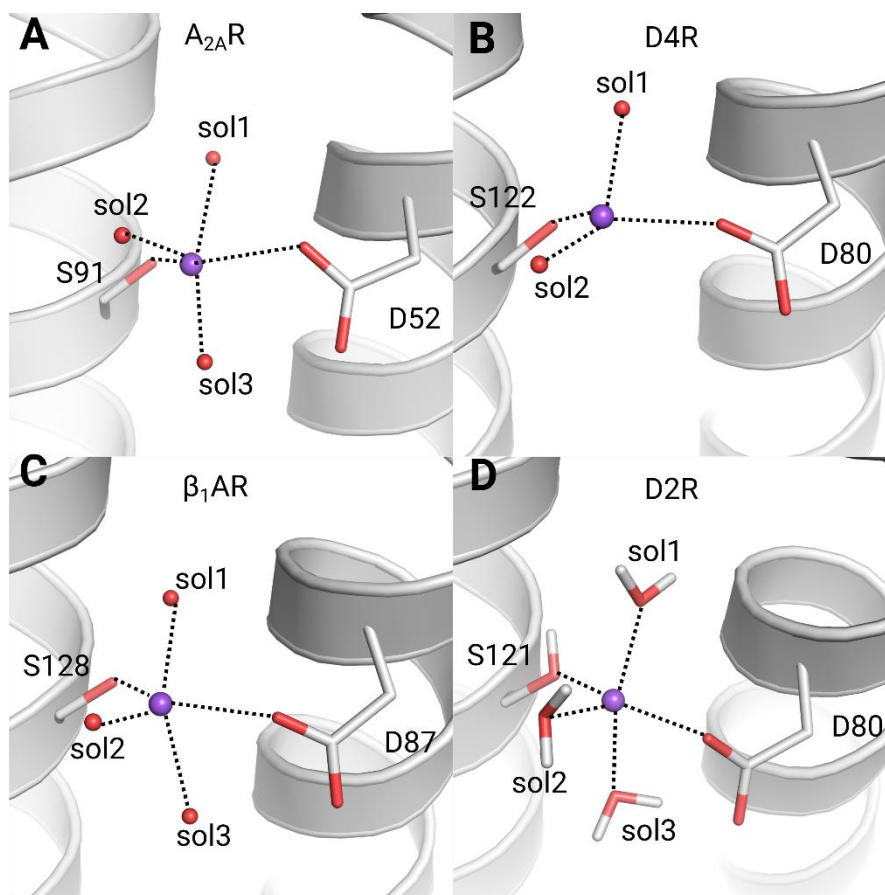* QM calculation of pKa of the hydroxyl group in quinolin-8-ol ring.

**Figure S1. The allosteric sodium ions observed in high resolution structures of GPCRs.** (a) $A_{2A}R$ (pdb code: 5NM4), (b) D4R (pdb: 5WIV) and (c) $\beta_1AR$ (pdb: 4BVN). (d) The final structure of apo-D2R obtained from MD simulations.
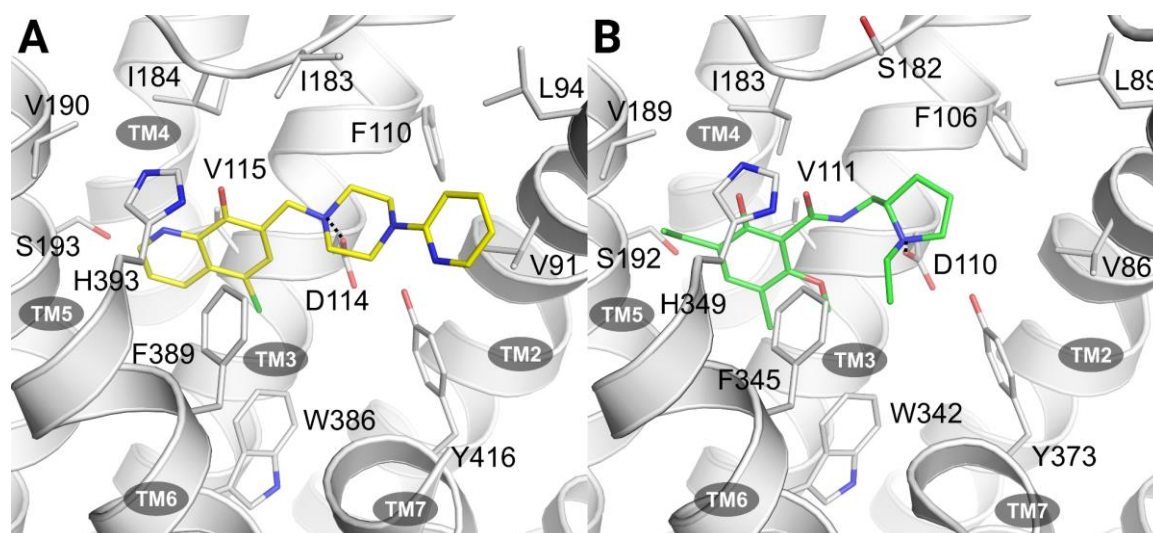
**Figure S2. Comparison of the binding modes.** (a) Docked agonist MLS1547 in D2R. (b) Crystal structure of D3R (pdb: 3PBL) showing the bound ligand ETQ. The binding modes are identical for both cases: (1) the left-hand side aromatic moiety in both ligands is located in an aromatic cage; (2) both ligands established an ionic interaction with residue $D^{3.32}$.
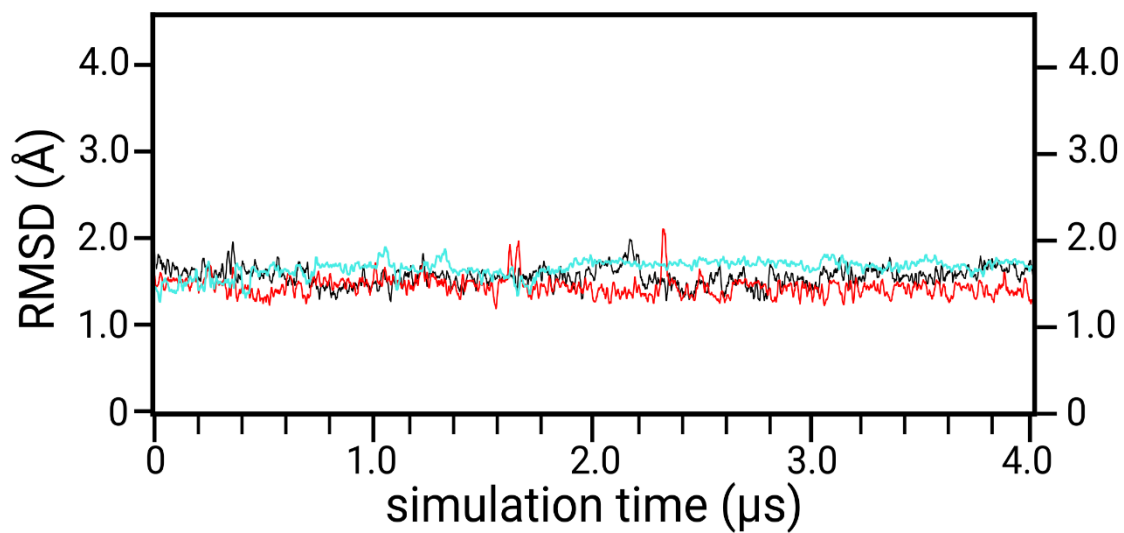
**Figure S3.** The root-mean-square deviation (RMSD) of MLS1547 during three different long-time scale MD simulations (in different colors). The fluctuation of MLS1547 was very small and the RMSD stabilized at about 1.5 – 1.7 Å.
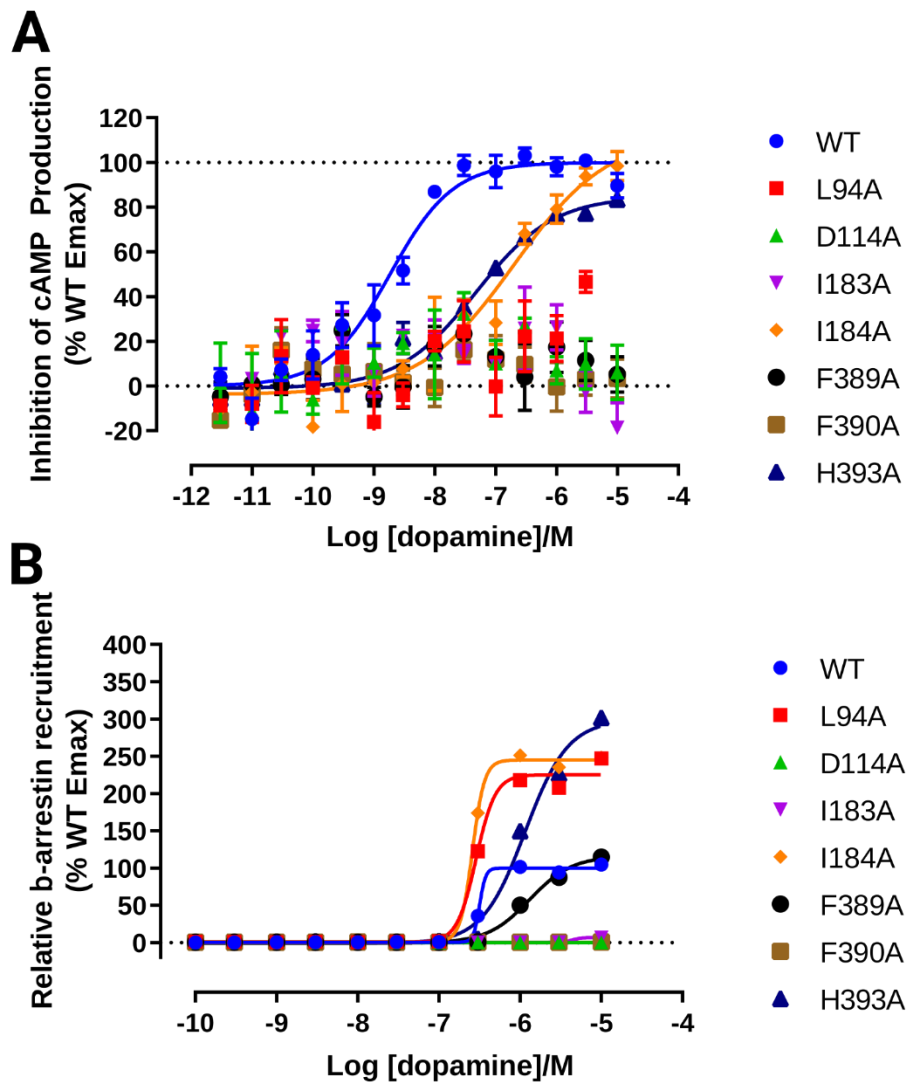
**Figure S4.** The dopamine activity against D2 receptor for (A) G protein activity and (B) β-arrestin activity. Mutation H393[6.55]A does not show significant influence for dopamine activity, implying that H393[6.55] does not play an essential role for the binding of dopamine.
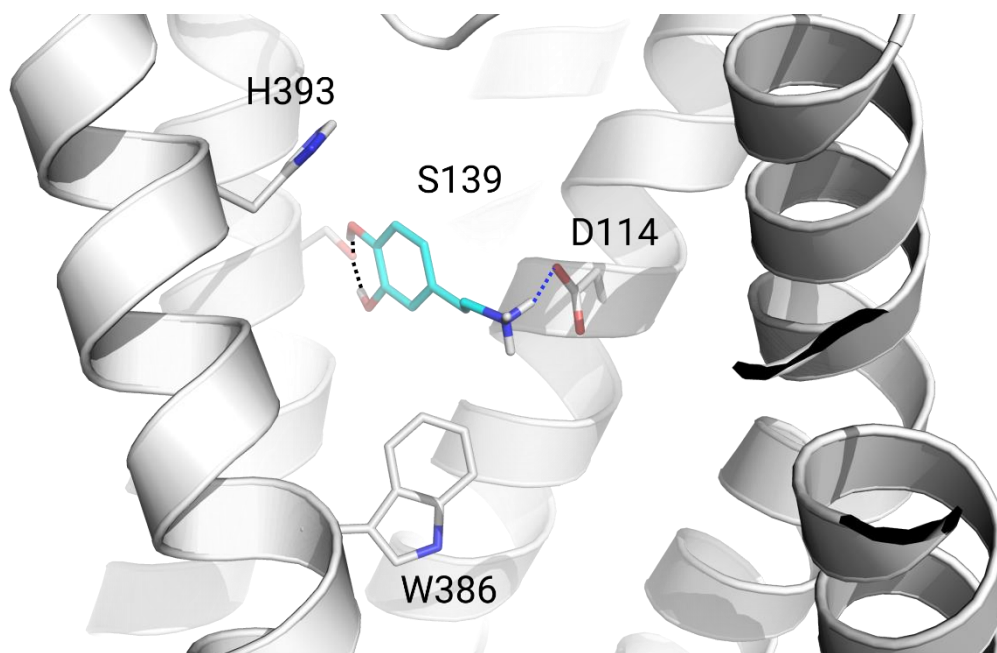
**Figure S5.** The binding mode of dopamine against D2R. Two hydrogen bonds (black dash) and one ionic interaction (red dash) were found between dopamine (cyan stick) and residues S139 and D114$^{3.32}$ (white stick) in D2R, respectively.
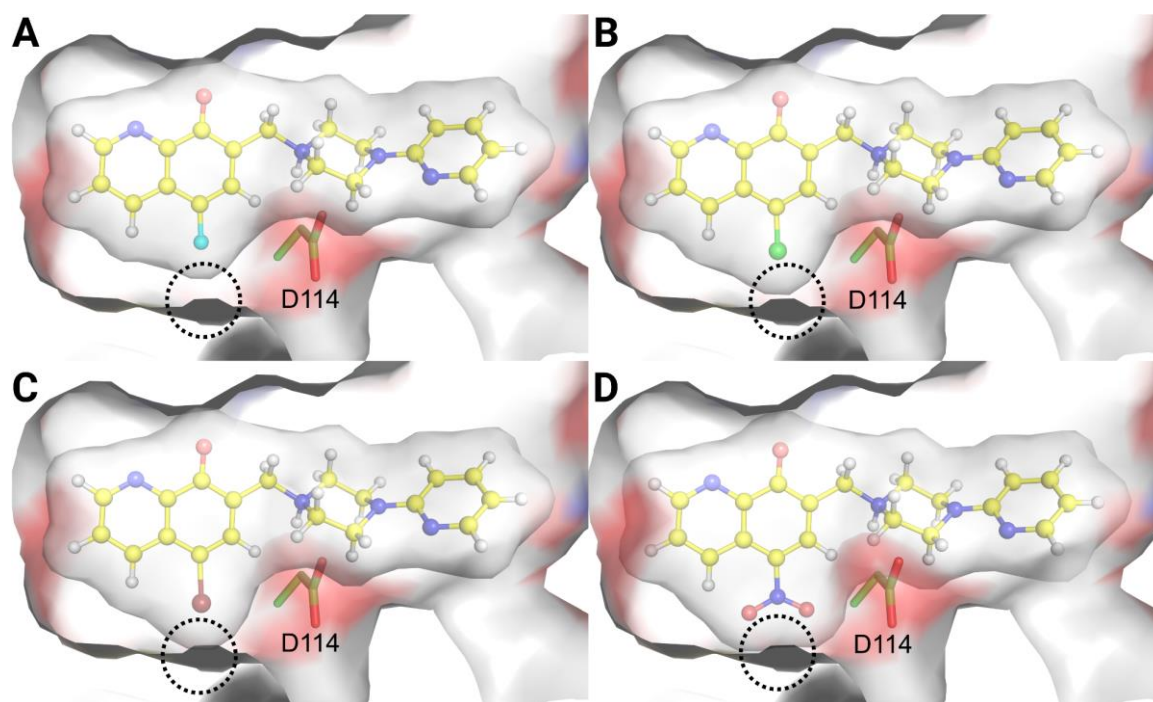
**Figure S6. The surface shape of MLS1547 and its chemically modified variants in the binding pocket.** (a) MLS-d1, (b) MLS1547, (c) MLS-d3 and (d) MLS-d4. Colored background surface indicates the binding pocket of D2R. White surface near compounds represent the molecular surface of each ligand. Yellow balls-and-sticks represent ligands. A fluorine in MLS-d1 fits very well into the binding pocket of D2R; it is located far away from the negatively charged D114[3.32]. The chlorine in MLS1547 experiences small steric repulsion in the binding pocket. Both bromine in MLS-d3 and the nitryl group in MLS-d4 do not fit well into the binding pocket. Further, both are located too close to the negatively charged D114[3.32].
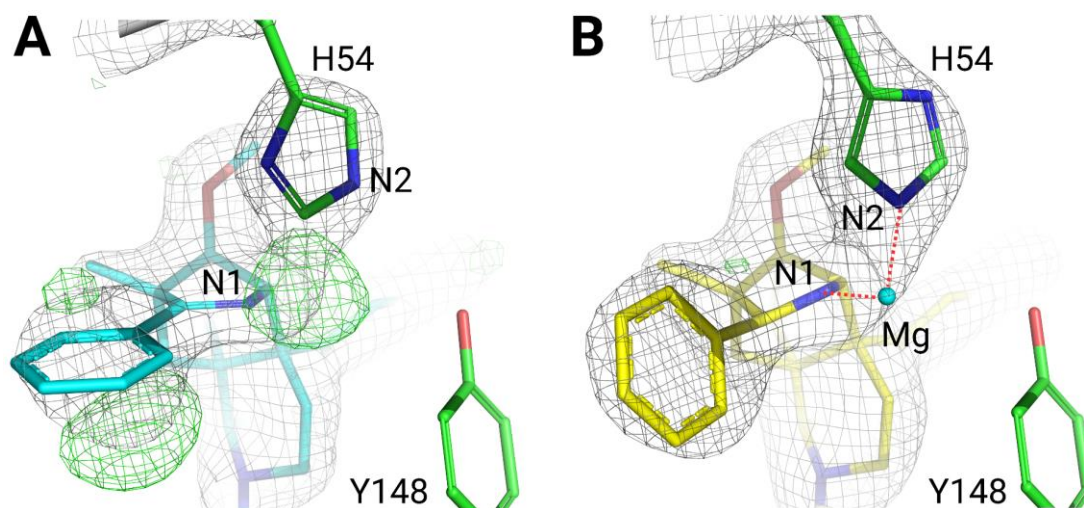
**Figure S7.** A Mg2+ ion was found in the high-resolution crystal structure of μ-opioid receptor (μOR, PDB: 5C1M). (A) The "unidentified" electron density map in the orthosteric binding site μOR. Green grid: Fo-Fc positive electron density map at 3.2 σ level which indicated missing atoms in the corresponding region. Gray grid: 2Fo-Fc electron density map at 1.2 σ level. (B) A refined crystal structure of μOR which is completed by an Mg$^{2+}$ ion. Mg$^{2+}$ ion established a coordinating interaction with both μOR and agonist BU72.
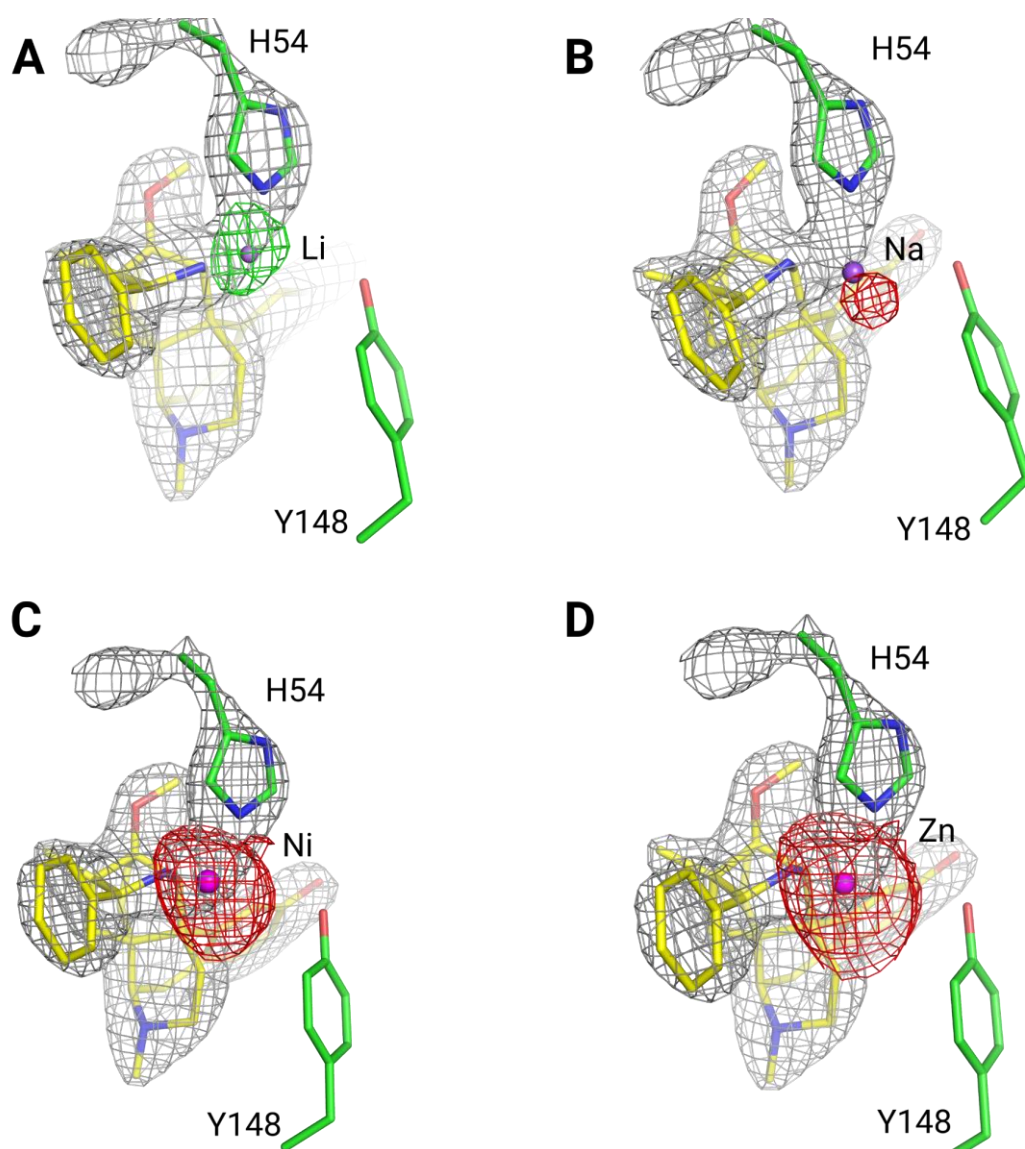
**Figure S8.** The refined electron density map of the "unidentified region" (pdb: 5C1M) for (A) Li+ (B) Na+ (C) Ni$^{2+}$ and (D) Zn$^{2+}$. Green grid: Fo-Fc positive electron density map at 3.2 σ level which indicated the missing atoms in the corresponding region. Gray grid: 2Fo-Fc electron density map at 1.2 σ level. The Li ion is too small to fit the "unidentified region" and a large Fo-Fc positive map is still there after refinement. Na, Ni and Zn ions are too big to fit into the "unidentified region" as indicated by the Fo-Fc negative electron density map after refinement. The ions themselves were so big that they were even repelled out of the 2Fo-Fc map.
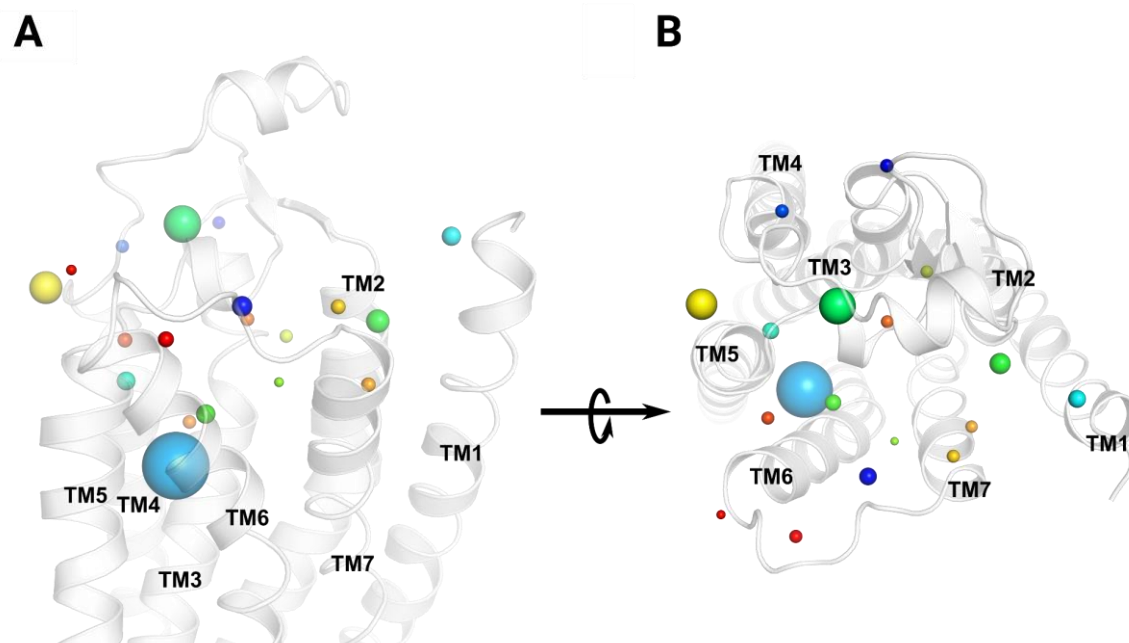
**Figure S9. His residues found in GPCR structures**. Different colors of spheres indicate different locations. The sizes of spheres are correlated to the frequency of their occurrence. The most His-rich region has been found in the vicinity of the orthosteric site next to TM5 and TM6 (dark cyan sphere).